J Toxicol Pathol 2014; 27: 73–80

Original Article

Absorption, Distribution and Pathological Injury in Mice Due to Ricin Poisoning Via the Alimentary Pathway

Na Dong[1, 2], Zheng Li[2], Qian Li[2], Junhua Wu[2], Peiyuan Jia[2], Yuxia Wang[2,*], Zhongcai Gao[2], Gang Han[2], Yifan Wu[2, 3], Jianping Zhou[2], Junjie Shan[2], Hua Li[2], Wenqing Wei[1,*]

[1] General Hospital of Beijing Military Command, Beijing 100700, China
[2] Beijing Institute of Pharmacology and Toxicology, Beijing 100850, China
[3] School of Medicine, Shanghai Jiaotong University, Shanghai 200025, China

Abstract: The aim of this work was to investigate the potential interactions between intestinal absorbance and ricin poisoning. The Caco-2 cell monolayer and everted intestinal sac (VEIS) models were used. The distribution of ricin in CD-1 mice intoxicated with 0.1 mg/kg of ricin intragastrically was determined by immunohistochemistry. The results showed that ricin could not transfer across the healthy Caco-2 cell monolayer within three hours after poisoning. However, it could pass through the everted rat intestinal wall after 0.5 h of incubation. The toxin in the liver, spleen, lungs and kidneys of mice could be detected as early as 1 h after intoxication. The pathological results were in accordance with the cytotoxicities of ricin in Caco-2, HepG 2, H1299 and MDCK cells, indicating that though no significant symptom in mice could be observed within 3 h after ricin intoxication, important tissues, especially the kidneys, were being injured by the toxin and that the injuries were progressing. (DOI: 10.1293/tox.2013-0049; J Toxicol Pathol 2014; 27: 73–80)

Key words: ricin, immunohistochemistry, alimentary poisoning

Introduction

Ricin, a powerful cytotoxic protein derived from the seeds of the castor oil plant, consists of two polypeptide chains named ricin toxin A chain (RTA) and ricin toxin B chain (RTB) linked via a disulfide bridge[1]. RTB mediates the binding to glycolipids or glycoproteins on the cell surface via its lectin receptors, followed by endocytic uptake into the cell[2]. After endocytosis, ricin is transported retrogradely from endosomes to the Golgi and further on to the endoplasmic reticulum (ER), which is its unique trafficking pathway in the cell. As a potent toxin, ricin kills eukaryotic cells by inhibiting protein synthesis, inducing serious intoxication symptoms in poisoned people. Both antibodies and competitive ligands have been used to intervene in the binding of the toxin to cells[3]. The morbidity and mortality of ricin is dependent upon the route of exposure. When ingested, ricin causes severe gastrointestinal symptoms followed by gastrointestinal hemorrhage with hepatic, splenic and renal necrosis. There is a latent period of more than 8 hours post ingestion after oral exposure before the symptoms of poisoning are observed in animal models.

Research into antitoxins against ricin poisoning has attracted wide attention, including prophylactic and therapeutic strategies[4, 5]. More in-depth research on the trafficking and toxicity of ricin in animals is expected to shed light on its toxic mechanism and even contribute to prophylactic agent design and prediction of the therapeutic window for specific antidotes.

In this paper, we aimed to investigate the absorption and distribution process of ricin and to analyze the pathologic injury to mice during toxic symptom latency. In order to evaluate the intestinal absorption process in mice after ingestion of ricin, Caco-2 cells were used to establish a monolayer cell model to determine the absorption and transformation[6]. For a better understanding of ricin absorption, we also used the everted intestinal sac model[7, 8] to validate the uptake route of ricin from the gastrointestinal tract in Wistar rats. The cytotoxicity of ricin in Caco-2, HepG 2, H1299 and MDCK cells was determined to compare their sensitivity to ricin poisoning. The distribution of ricin in different tissues of mice intoxicated at different time points was determined by immunohistochemistry. So the monolayer cell model, the isolated and reverted intestine, and the mouse ingested model were used to analyze the absorption process of ricin. It will be helpful to explain the absorption, distribution and even intoxication of animals poisoned along the alimentary tract with reference to the results of pathological changes in

Received: 3 September 2013, Accepted: 19 December 2013
Corresponding authors: Y Wang (e-mail: wangyuxia1962@hotmail.com) and W Wei (e-mail: wqwei2000@qq.com)

the liver, kidney, lung, spleen and intestine induced by ricin.

Materials and Methods

Materials

The ricin used in this study was supplied by the Laboratory of Toxicant Analysis, Beijing Institute of Pharmacology and Toxicology. Human non-small lung cancer cell line H1299, human colon carcinoma cell line Caco-2, human hepatocellular liver carcinoma cell line HepG 2 and Madin-Darby canine kidney (MDCK) cells were obtained from the American Type Culture Collection (ATCC). Mouse ascites containing monoclonal antibodies (Mab 4C13 and Mab 3D74) were produced in the Beijing Institute of Basic Medical Sciences. The antibodies were purified using protein G sepharose 4 Fast Flow (Amersham), and Mab 4C13 was labeled with horseradish peroxidase (HRP) in our laboratory. Female CD1 mice and Wistar rats were supplied by Vital River Laboratory Animal Technology Co., Ltd. (SCXK [Jing] 2012-0001). They were housed in a controlled environment (21 ± 2°C; 55 ± 5% humidity; 12 h dark and light cycle with light provided between 6 am and 6 pm). Food and water were given *ad libitum*. All the animal experiments were carried out in the Beijing Center for Drug Safety Evaluation and in accordance with a protocol approved by the Institutional Animal Care and Use Committee of the Center,which is in compliance with the guidelines of the Association for Assessment and Accreditation of Laboratory Animal Care International (AAALAC).

Cell culture

Cells were cultured in a MEM/EBSS medium supplemented with fetal bovine serum (FBS, GIBCO, 20% for Caco-2 cells and 10% for HepG 2, H1299 and MDCK cells), 1% nonessential amino acids, 100 units/ml penicillin and 100 μg/ml streptomycin and incubated at 37°C in the presence of 5% CO_2. Cells were subcultured when they reached approximately 80% confluence.

Cell viability assay

First of all, Caco-2, HepG 2, H1299 and MDCK cells were seeded in 96-well cell culture plates at a density of 1×10^5 cells/well in complete medium supplemented with 20% or 10% FBS. After incubation, the cells were washed with serum-free medium and cultured with different concentrations of ricin (1, 10, 100 and 1000 ng/ml) diluted with serum-free medium. Cells cultured with 0 ng/ml of ricin were used as the normal control. At the designated time point (0.5, 1, 3, 6, 24 and 48 h), 3-(4, 5-dimethylthiazol-2-yl)-2, 5-diphenyltetrazolium bromide (MTT) was added to each well. After 4 hours of incubation at 37°C, 150 μL dimethyl sulfoxide (DMSO) was added to dissolve formazan crystals completely for about 15 minutes at room temperature after the medium was removed. Absorbance at 490 nm was measured with a micro-ELISA reader (Varioskan Flash version 2.4.3, Thermo Scientific, Waltham, MA, USA). The optical density of samples without ricin (cells only) was set at 100%. The viability ratio of cells treated with ricin was calculated as:

$$\text{Viability ratio} = A490_{sample}/A490_{control}.$$

Cell differentiation and transport of ricin across Caco-2 monolayer

Caco-2 cells were seeded in polycarbonate inserts with a pore diameter of 0.4 μm (24-well Millicell® Hanging Cell Culture Inserts, Millipore, Darmstadt, Germany) at a density of 3×10^5 cells/well in complete medium supplemented with 20% FBS. The media volumes were 0.45 ml and 0.6 ml in the apical (AP) and basolateral (BL) compartments, respectively. The media on both sides was replaced every other day. The cells were cultured in an incubator at 37°C with 5% CO_2 and allowed to differentiate for 21 days. The baseline transepithelial electrical resistance (TEER) value of the inserts was more than 550 Ω/cm^2, representing good monolayer integrity[9]. Media on both sides of the compartments were aspirated, and the compartments were washed twice with Hanks balanced salt solution (HBSS, NaCl 136.9 mM; KCl 5.4 mM; $Na_2HPO_4{\cdot}H_2O$ 0.3 mM; Hepes Free Acid 25.2 mM; pH 7.2–7.4). The cells were incubated in HBSS at 37°C for 20 min in order to balance their internal environment, and 0.35 ml aliquots of 0, 1, 10, 100, 1000 and 10,000 ng/ml of ricin in HBSS were added to AP compartments; 1.4 ml HBSS aliquots were added to BL compartments. We also added 0, 100 and 10,000 ng/ml of ricin in HBSS into AP compartments without Caco-2 cell culturing to see whether ricin could permeate the well base directly. At different time points (15, 30, 60, 90, 120 and 180 min) after ricin administration, 120 μL samples from the BL compartment were transferred to conical centrifuge tubes, and the same volume of fresh HBSS buffer was added to the compartment. At the end of the experiment, all the remaining samples were removed. All samples collected were stored at –20°C until they were analyzed by sandwich enzyme-linked immunosorbent assay (ELISA).

Establishment of the everted intestinal sac model

After 12 h of fasting, female rats weighing 200–250 g were anesthetized with an overdose of ether and euthanized. The duodenum, jejunum, ileum and colon segments were removed and washed with Kreb's solution (118.0 mM NaCl, 4.7 mM KCl, 2.5 mM $CaCl_2$, 25.0 mM $NaHCO_3$, 1.2 mM KH_2PO_4, 1.2 mM $MgSO_4$, 11.1 mM glucose). The soft end of a homemade silicone casing tied around the end of a plastic cannula was put into the intestine with silk thread ligaturing, and the intestine was flipped carefully before the inside intestine was washed with the Kreb's solution. The everted part was cut into 5 cm segments. The other end of the intestine was closed by ligature. The intestinal sac was then immersed into a Maxwell bath tube filled with 60 ml of 10 μg/ml ricin in Kreb's solution at 37°C and supplied with mixed gas containing 95% O_2 and 5% CO_2. Two milliliters of Kreb's solution was injected into the intestine to balance for 5 min. Sample aliquots (22 μl) were removed from the intestinal sac at the time points of 15, 30, 45, 60, 90, 120, 150

and 180 min, respectively, and an equal volume of Kreb's solution was replenished after each sampling. The removed samples were stored at –20°C until measurement by ELISA.

Sandwich ELISA to analyze ricin in the samples

ELISA was performed as described previously[10, 11]. Different epitopes could be recognized by Mab 3D74 and Mab 4C13. We used Mab 3D74 and Mab 4C13 labeled with HRP to establish the ELISA for ricin detection. Ricin could be captured by Mab 3D74 coated on enzyme immunoassay (EIA) plates (96-well, Costar) and then detected by HRP-labeled Mab 4C13 with the sensitivity limit of 2.5 ng/ml ricin in PBST, serum and water[12]. Briefly, the plates (96-well, Costar) were coated with Mab 3D74 (400 ng/well) and then incubated with samples before HRP-labeled 4C13 was added. Ricin was detected by measuring the activity of HRP conjugated to 4C13 colorized with tetramethylbenzidine (TMB) substrate.

Establishment of an intoxicated animal model

Female CD1 mice (body weight 20 to 22 g) were used for the experiment. After 12 h of fasting, animals were intragastrically administered ricin at a dose of 0.1 mg/kg of body weight. The ricin was diluted with saline to a concentration of 0.01 mg/ml. The intoxicated mice received 0.1 ml of ricin/10 g body weight. Mice in the control group (n=4) were intragastrically administered saline. At the designated time points (1, 3 and 6 h) postexposure, the plasma samples were separated, and the nephrotoxicity and hepatotoxicity related to biochemical indicators were detected by a biochemical analyzer (Hitachi 7180) at the National Beijing Center for Drug Safety Evaluation and Research. Proximal small intestine, liver, spleen, lung, and kidney samples were dissected out and fixed in 10% formalin.

Immunohistochemistry to trace ricin distributed in mouse tissues

The proximal small intestine, liver, spleen, lung and kidney were fixed in 10% formalin for 24 h prior to processing and paraffin embedding. Sections 3 μm thick were prepared and analyzed by immunohistochemistry. Monoclonal antibody 4C13 has been used to immunoprecipitate ricin or RTA in the tissues of poisoned mice and to analyze the toxin in detoxified meal of castor beans by Western blotting[10, 13]. For analysis of ricin, sections were prepared and analyzed by immunohistochemistry using Histostain™-Plus Kits (Zymed Laboratories, San Francisco, CA, USA), Mab 4C13 (1 μg/ml) and the peroxidase-conjugated goat anti-mouse IgG (1/1000, Wuhan Boster Biological Technology, Ltd., Wuhan, China). Tissue processing, embedding, sectioning and staining were performed at SOONBIO Technology Corporation.

Histopathological analysis

Tissue samples of the proximal small intestine, liver, spleen, lungs and kidneys were dissected out and fixed in 10% formalin. Sections 3 μm thick were prepared and stained with hematoxylin and eosin. Microscopic observation was performed under a Leica DMI3000 B fluorescence microscope, and photographs were taken using Leica Application Suite V3.

Results

Ricin-induced cytotoxicity in Caco-2, HepG 2, H1299 and MDCK cells

The cytotoxicity induced by ricin in Caco-2, HepG 2, H1299 and MDCK cells was determined by MTT assay (Fig. 1). Cells were treated with serial dilutions of ricin for different lengths of time. The results indicated that there was little change in the survival rate of Caco-2 cells when they were treated with ricin for 0.5 to 6 h. However, the survival rate decreased significantly when cells were treated with the toxin for 24 h and 48 h. The survival rate decreased to between 60% and 70% when cells were treated with 1 μg/ml of ricin for 24 h and 48 h. The cells treated with 1 to 1000 ng/ml of ricin exhibited almost the same survival levels, indicating that 1 ng/ml ricin could reach the highest level of cytotoxicity. Compared with Caco-2 cells, HepG 2, H1299 and MDCK cells exhibited high sensitivities to ricin. After treatment with 10 ng/ml of ricin for 48 h, 60% of Caco-2 cells, 50% of HepG 2 cells, 25% of H1299 cells and 13% of MDCK cells survived.

Permeation of ricin across Caco-2 monolayer measured by sandwich ELISA

Ricin can be taken up by endocytosis. It is unknown whether ricin can transfer through the intestinal epithelium via the paracellular route. We used Caco-2 monolayers to represent the intestinal epithelium and collected the samples from the BL compartments for ricin determination by ELISA. When 100 ng/ml of ricin was directly loaded into a cell-free insert, about 1 ng/ml of ricin, which was lower than the limit of detection, was detected in samples from the BL compartments. However, when 10 μg/ml of ricin was loaded, the signal of ricin transportation across the insert base was significantly increased (Fig. 2A). These data indicated that ricin could be well absorbed by the polycarbonate insert, which would decrease the concentration of ricin in the BL compartment, especially when a low concentration of ricin was loaded. However, when we loaded 10 μg/ml of ricin on Caco-2 cell monolayers, no ricin was measured in the BL compartment even at 180 minutes postexposure (Fig. 2B).

Detection of ricin absorption through the intestine using the everted intestine sac model

The everted intestine sac model has been well used in the research of drug absorption and metabolism[14]. We established an intestine sac model to determine the ricin in the internal sac after the everted intestine was immersed in a high concentration of ricin for different lengths of time. The results in Fig. 3 showed that ricin could pass through the everted intestine within 1 h. The main sections were the

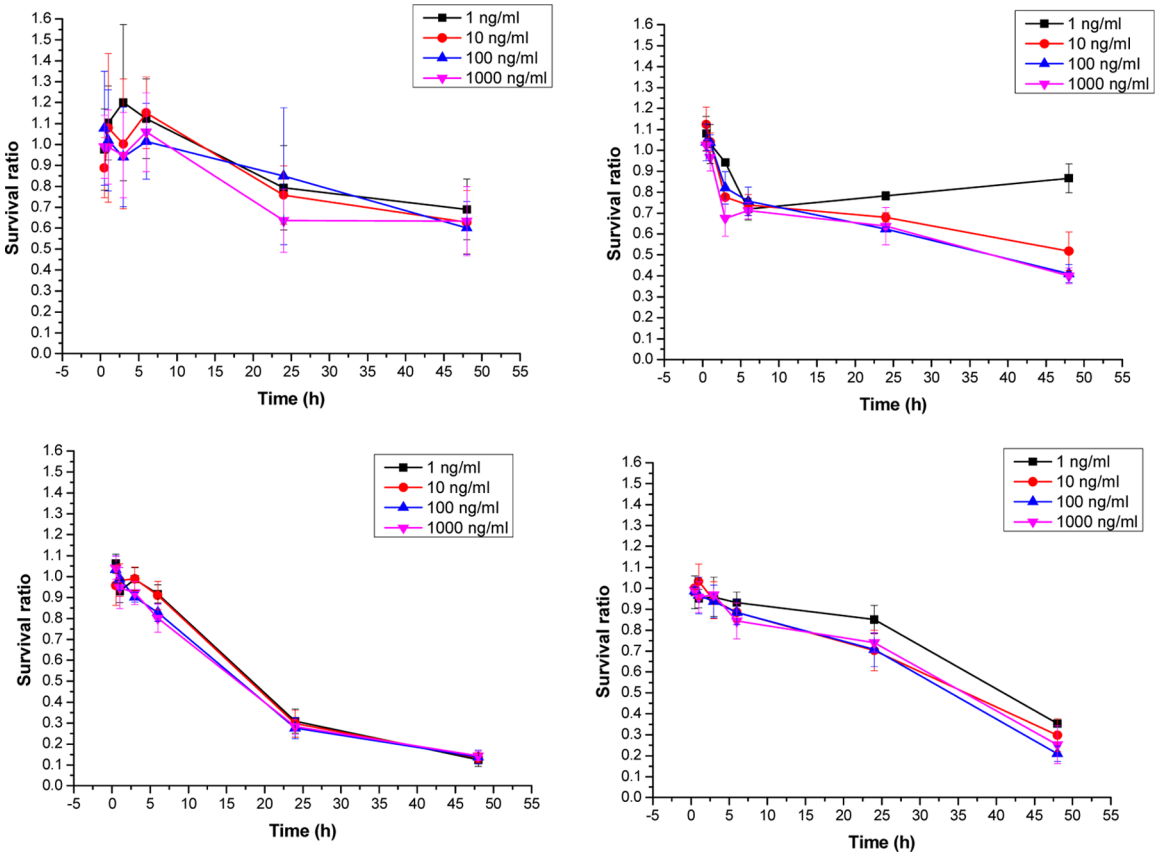

Fig. 1. Cytotoxicity induced by different concentrations of ricin. Cells were treated with different concentrations of ricin. The value of absorbance at 490 nm was detected at 0.5, 1, 3, 6, 24 and 48 h after ricin treatment by MTT assay. A, Caco-2 cells; B, HepG 2 cells; C, MDCK cells and D, H1299 cells. Data are means ± SD (n=10).

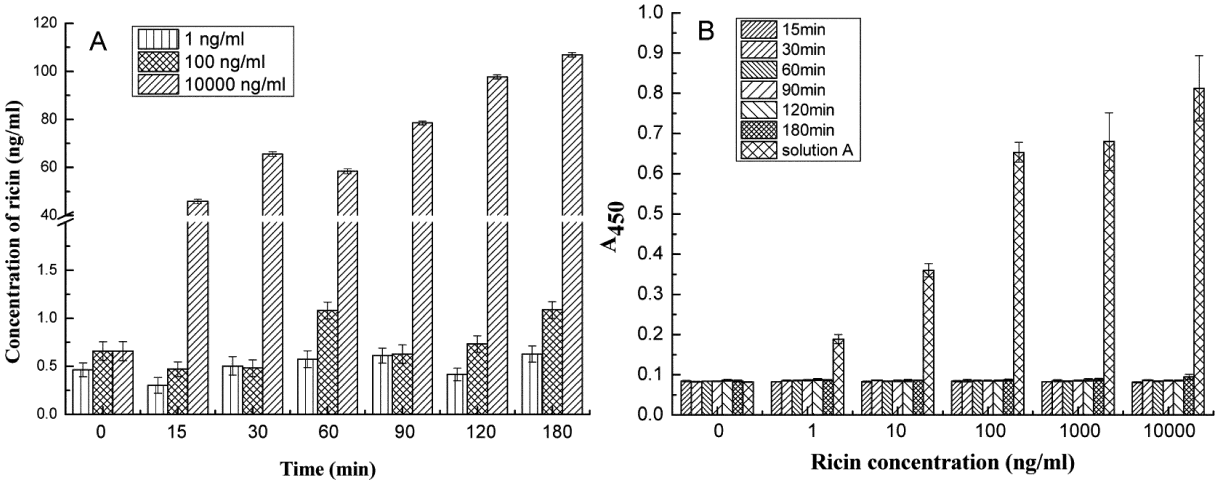

Fig. 2. The detection of ricin passed through the basement membrane of an insert cultured with or without Caco 2 cells. (A) Ricin at 1 ng/ml, 100 ng/ml or 10 μg/ml was loaded onto the basement membrane of an insert directly. The concentration of ricin in the solution in the BL compartment was determined by ELISA. (B) Different concentrations of ricin were respectively loaded onto the basement membrane of an insert cultured with Caco 2 cells. Ricin samples from the BL compartments and in solution A from the AP compartment were detected at the same time. All values are expressed as means ± SD (n=4).

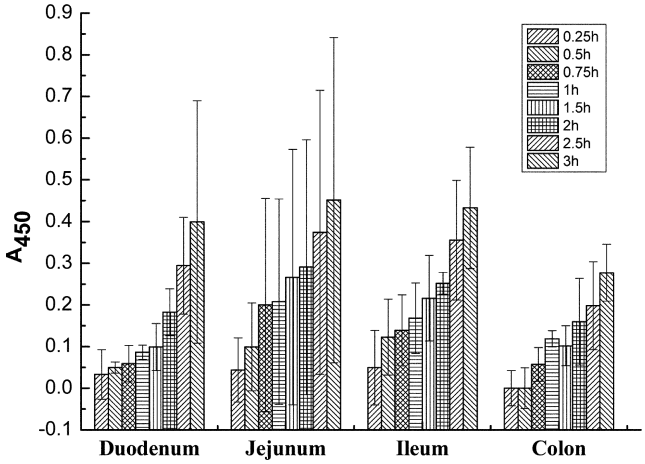

Fig. 3. Ricin absorbed through the intestine wall in the everted intestine sac model. The A450 values were determined after the everted intestine sac was immersed into 10 μg/ml ricin in Kreb's solution. Sandwich EILSA was used. All data are expressed as means ± SD (n=4).

jejunum and ileum.

We have mentioned that ricin could not pass through monolayer Caco-2 cells even at the high concentration of 10 μg/ml (Fig. 2B). In this experiment, when the intestine sac was immersed in the same concentration of ricin, the toxin could be detected in the opposite part of the intestine wall, indicating that the toxin could not be transferred through the intestine wall through cells directly but could be transferred through the blood vessels, which was not distributed in the monolayer cell model.

Toxin in different tissues of mice poisoned with ricin along the alimentary tract

When ricin is administrated intragastrically, it should be absorbed into the blood circulation and then distributed in different tissues of organs. The intestine must be the main tissue for its absorption along the alimentary tract, but what we need to find out is whether it is the main section for toxin distribution and how fast it accumulates in important organs. We gave mice a lethal dose of ricin and collected the lungs, liver, kidneys, spleen and proximal small intestine to examine the toxin with a specific antibody against ricin by immunohistochemistry (Fig. 4A). The results showed that ricin could penetrate into the lung, liver, kidney and spleen quickly through the blood circulation. Ricin could be colorized in these tissues at even 1 h after intoxication. In the intestine samples of mice intoxicated for 1, 3 or 6 h, only slightly tinted brown spots were found, and at 24 h, a large number of dark brown spots appeared. It seems that ricin enters intestine cells slowly even if the intestine is the major tissue exposed to ricin via alimentary intoxication.

Pathological analysis of tissues of mice intoxicated with ricin by intragastric administration

As shown in Fig. 4B, apparent injury to the liver and kidneys of poisoned mice was observed as early as 1 h after toxin treatment. The liver cells were considerably swollen, with their structures damaged and the density different from normal after poisoning for 1, 3, 6 or 24 h. The renal glomerulus showed hemorrhage, and some endothelial cells of vessels of the kidneys were absent. The renal pelvis was bleeding, and edema was observed in renal tubule cells. These symptoms deteriorated with the passage of time. In the spleen, widespread hemorrhage was found. However, there were few lesions in the proximal small intestine compared with the toxic changes in the kidneys. We have mentioned that kidney cells might be more sensitive to ricin than intestine cells. This result was also concordant with the distribution of ricin in different tissues of mice after ricin poisoning. At 24 h after poisoning, the mice developed a mild to moderate necrotizing pneumonia, with slight interstitial edema and diffuse perivascular inflammation.

Biochemical analysis of serum samples of mice

At 3 h after ricin intoxication, the serum samples of mice were examined to evaluate nephrotoxicity and hepatotoxicity. The results in Table 1 summarize some of the related parameters in blood. At 3 h after ricin treatment, the activities of alanine aminotransferase (ALT) and aspartate aminotransferase (AST) were significantly higher than those of the control, being consistent with the results of rats poisoned with ricin reported by Balint. His results indicated that the serum ALT and AST values were significantly increased compared with the control after 24 h ricin exposure by the i.p. route[15]. The elevated creatinine (CREA) level indicated the decline of the glomerular filtration rate, and the high creatine kinase activity (CK) suggested the possibility of myocardiolysis induced by ricin poisoning. A preliminary study of Kumar *et al*. revealed the same hepatotoxicity and nephrotoxicity in mice at 24 h post ricin via i.p. treatment[16]. Whether the decreased level of BUN was related to the inhibition of protein synthesis and metabolism requires the further investigation.

Discussion

Ricin has the potential to be one of the most used toxins by terrorists. Basically, the clinical syndrome resulting from ricin poisoning is dependent on the route of exposure[17]. It is generally believed that aerosolized ricin is the most lethal route of exposure. Certainly the oral and injection routes can also pose a significant risk to humans[17–19]. The obvious symptoms of ricin poisoning do not appear for hours, but gastrointestinal bleeding, liver necrosis, diffuse nephritis and diffuse splenitis would be likely to emerge systemically after the latency period[20].

In this study, we determined the cytotoxicity of ricin in Caco-2, HepG 2, H1299 and MDCK cells. The results indicated that MDCK and H1299 cells were more sensitive

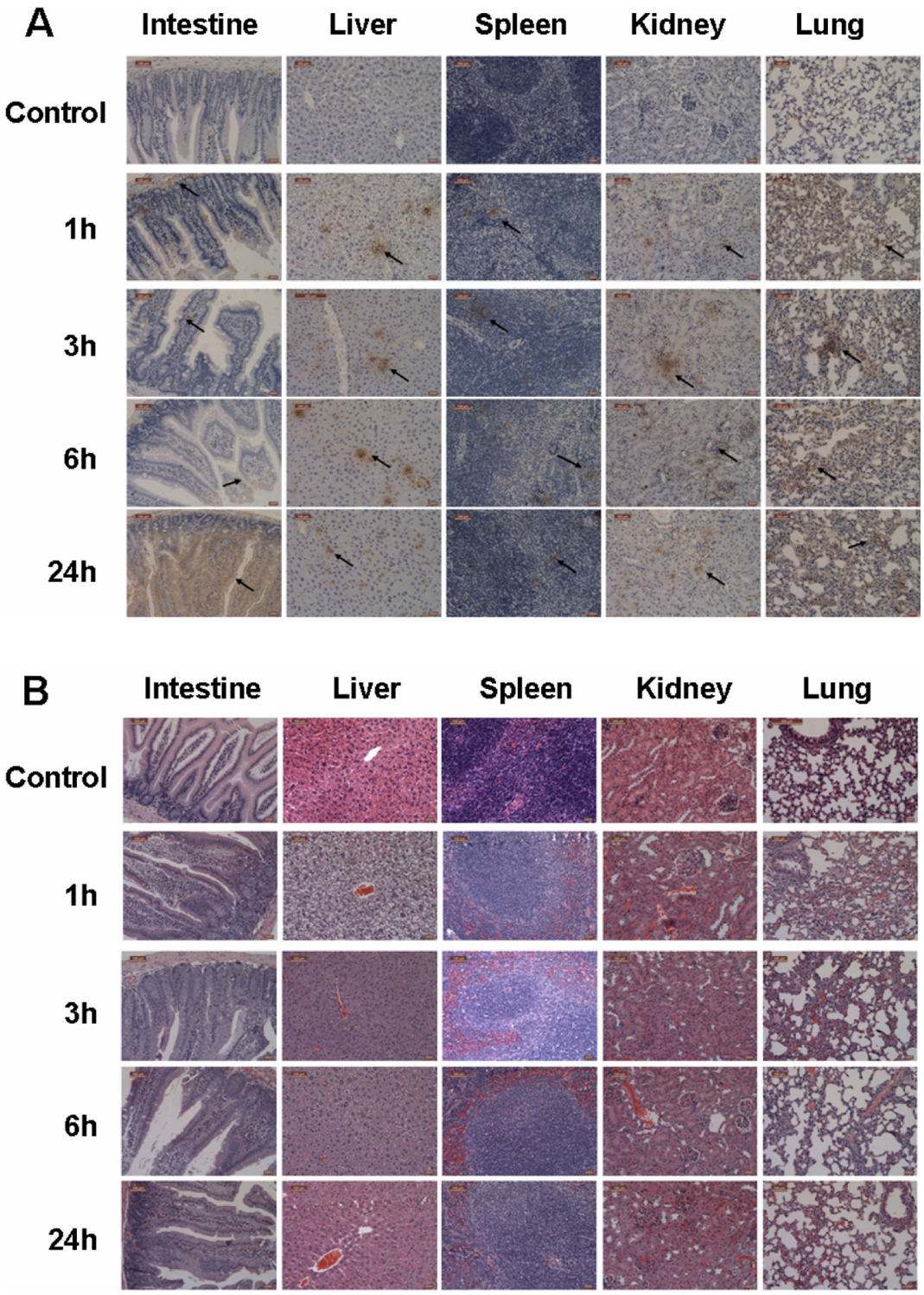

Fig. 4. Ricin accumulation and histopathological changes in the tissues of alimentary poisoned mice. The tissues of mice were harvested at different time points of intoxication. (A) Ricin was colorized by immunohistochemistry with monoclonal antibody (4C13) against ricin. Arrows represent the positive signals. (B) Pathological lesions in tissues were determined. Microscopic observation was performed on sections of tissue samples under a Leica DMI3000 B fluorescence microscope, and photographs were taken using Leica Application Suite V3. Original magnification × 20.

to ricin exposure, and this could be due to (1) the glycoprotein or glycolipids on the surface of cells, which facilitate the entry of ricin, and (2) the P-glycoprotein expression on the cell membrane, which could pump ricin out of cells. Our results showed that ricin could pass through the everted intestinal sac *in vitro* and be quickly transmitted to

Table 1. Effect of Ricin on Nephrotoxicity- and Hepatotoxicity-related Biochemical Indicators in Sera of Mice

Parameters	Control	Ricin intoxicated
ALT (U/L)	95.20 ± 15.16	161.00 ± 61.93 *
AST (U/L)	189.60 ± 35.11	279.00 ± 28.77 **
ALP (U/L)	299.80 ± 46.26	317.00 ± 90.29
TP (g/L)	49.7 ± 1.73	46.58 ± 6.49
ALB (g/L)	39.04 ± 1.58	36.10 ± 5.44
TCHO (mM)	3.25 ± 0.29	2.98 ± 0.35
BUN (mM)	12.36 ± 1.22	8.63 ± 1.51 **
TBIL (μM)	1.66 ± 0.15	2.13 ± 0.33 *
GLU(mM)	8.98 ± 1.35	3.05 ± 1.12 **
TG (mM)	0.746 ± 0.11	0.85 ± 0.18
CREA (μM)	13.72 ± 2.61	17.50 ± 0.88 **
CK (U/L)	1946.20 ± 524.94	3539.75 ± 778.71 **

Alanine aminotransferase (ALT), aspartate aminotransferase (AST), alkaline phosphatase (ALP), total protein (TP), albumin (ALB), total cholesterol (TCHO), blood urea nitrogen (BUN), total bilirubin (TB), glucose (GLU), triglycerides (TG), creatinine (CREA) and creatine kinase (CK) in mouse sera were determined. Data are expressed as means ± SD (n=5). $^{*}p<0.05$ compared with the normal control; $^{**}p<0.01$ compared with the normal control. Significant differences were determined using SPSS 13.0.

the liver, kidneys, spleen and lungs of mice intoxicated by gastric gavage *in vivo*. However, no ricin transmission was determined through Caco-2 cell monolayers. Previous research showed that the major disadvantage of Caco-2 cells was their low transportation rate. This research showed that Caco-2 cells were generally 20–40 times less permeable than cells of the normal human colon and 6–100 times less permeable than cells from the rat intestine[21]. We presumed that the ricin transported through tight junctions and exocytosis from cells was absorbed by the basement membrane of the polycarbonate insert. Although the Caco-2 cell monolayer has been widely used to evaluate the transport of small molecules across the intestinal barrier, the absorption of compounds by the insert should be taken into consideration when bigger molecules, like proteins, are evaluated. Mantis *et al*. determined the effect of reducing RTA with IgA Mabs on the transepithelial transportation of ricin[22]. In their research, MDCK II cells were used to establish monolayers, and the transport of biotinylated ricin was measured at 18 h after intoxication. In our research, we observed that after being cultured in serum-free medium for more than 4 h, the tight junction of Caco-2 cells became noncohesive, providing a pathway for ricin transport. In order to examine the ricin transportation through the normal intestine, the experiments were carried out within 3 h of ricin treatment. It was interesting that ricin could quickly pass through the everted intestinal sac, indicating that the internalized ricin could be secreted by exocytosis because the cell junctions are very tight and represent only 0.1% of the surface area of the intestine[23]. The results of the test in vivo also exposed the slow accumulation of ricin in the intestine compared with the ricin distribution in the liver, lungs and kidneys. The pathological assay showed that the liver and kidney were most damaged in the initial period of intoxication. This result could be partly evaluated by their abundant blood supply and responsibilities for metabolism and excretion of ricin. The sensitivity of different cells to ricin exposure should be considered. Previous research showed that ricin exerts its toxicity on many different cell types, making it impossible to pinpoint the exact cause of death[24]. Our experiment *in vitro* indicated that intestine cells were not as sensitive as other tissue cells to ricin poisoning even though they were treated with the same concentration of toxin. This was also found in the experiment *in vivo*. Although the intestine was the first tissue intoxicated with ricin, by gastric gavage, the kidney exhibited injury at 1 h after intoxication, which appeared much faster than the damage to the intestine.

It was previously reported that it took at least 6 h to traffic a significant amount of ricin from the mouse stomach to the blood stream[20]. Indeed, the absorption and distribution of ricin depend on many factors. Some physiological factors, such as gastric emptying and intestinal transit, also influence absorption. Our results of immunohistochemistry showed that ricin began to accumulate in the liver, spleen, kidneys and lungs at only 1 h post exposure in accordance with the pathological damage observed. This result indicated that although there were no significant toxic symptoms within several hours post intoxication, some important tissues were being injured and that the injuries were progressing; these injuries appeared much earlier than diarrhea induced by the injury to the intestine. Attention must be paid to the impairment of the liver and kidneys even in the initial stage of poisoning, and necessary symptomatic treatment needs to be provided to humans afflicted with ricin intoxication.

Acknowledgments: This work was supported by Grants from the National Basic Research Program of China (NO. 2010CB933904), the Shanghai Pujiang Talent Plan Program (11PJ1408800) and the Opening Project of the Shanghai Key Laboratory of Complex Prescription (Shanghai University of Traditional Chinese Medicine) (11DZ2270900).

References

1. Audi J, Belson M, Patel M, Schier J, and Osterloh J. Ricin poisoning: a comprehensive review. JAMA. **294**(18): 2342–2351. 2005. [Medline] [CrossRef]
2. Sandvig K, Torgersen ML, Engedal N, Skotland T, and Iversen TG. Protein toxins from plants and bacteria: probes for intracellular transport and tools in medicine. FEBS Lett. **584**(12): 2626–2634. 2010. [Medline] [CrossRef]
3. Thomas RJ. Receptor mimicry as novel therapeutic treatment for biothreat agents. Bioeng Bugs. **1**(1): 17–30. 2010. [Medline] [CrossRef]
4. Smallshaw JE, Richardson JA, and Vitetta ES. RiVax, a recombinant ricin subunit vaccine, protects mice against ricin delivered by gavage or aerosol. Vaccine. **25**(42): 7459–7469. 2007. [Medline] [CrossRef]
5. Stechmann B, Bai SK, Gobbo E, Lopez R, Merer G, Pinchard S, Panigai L, Tenza D, Raposo G, Beaumelle B, Sauvaire D, Gillet D, Johannes L, and Barbier J. Inhibition

of retrograde transport protects mice from lethal ricin challenge. Cell. **141**(2): 231–242. 2010. [Medline] [CrossRef]
6. Sandvig K, Prydz K, Hansen SH, and van Deurs B. Ricin transport in brefeldin A-treated cells: correlation between Golgi structure and toxic effect. J Cell Biol. **115**(4): 971–981. 1991. [Medline] [CrossRef]
7. Barthe L, Woodley J, and Houin G. Gastrointestinal absorption of drugs: methods and studies. Fundam Clin Pharmacol. **13**(2): 154–168. 1999. [Medline] [CrossRef]
8. Kilic FS, Batu O, Sirmagul B, Yildirim E, and Erol K. Intestinal absorption of digoxin and interaction with nimodipine in rats. Pol J Pharmacol. **56**(1): 137–141. 2004. [Medline]
9. Coyuco JC, Liu Y, Tan BJ, and Chiu GN. Functionalized carbon nanomaterials: exploring the interactions with Caco-2 cells for potential oral drug delivery. Int J Nanomedicine. **6**: 2253–2263. 2011. [Medline]
10. Men J, Lang L, Wang C, Wu J, Zhao Y, Jia PY, Wei W, and Wang Y. Detection of residual toxin in tissues of ricin-poisoned mice by sandwich enzyme-linked immunosorbent assay and immunoprecipitation. Anal Biochem. **401**(2): 211–216. 2010. [Medline] [CrossRef]
11. Leith AG, Griffiths GD, and Green MA. Quantification of ricin toxin using a highly sensitive avidin/biotin enzyme-linked immunosorbent assay. J Forensic Sci Soc. **28**(4): 227–236. 1988. [Medline] [CrossRef]
12. Lang L, Wang Y, Wang C, Zhao Y, Jia P, and Fu F. Determination of ricin by double antibody Sandwich enzyme-linked immunosorbent assay in different samples. J Inter Pharma Res. **36**: 12–16. 2009.
13. Wu J, Li Q, Dong N, Wang Y, Jia P, Liang X, and Zhao Y. Detection of residual ricin in the detoxified meal of castor beans. Mil Med Sci. **37**: 62–65. 2013.
14. Wilson TH, and Wiseman G. The use of sacs of everted small intestine for the study of the transference of substances from the mucosal to the serosal surface. J Physiol. **123**(1): 116–125. 1954. [Medline]
15. Balint GA. Ultrastructural study of liver cell damage induced by ricin. Exp Toxicol Pathol. **52**(5): 413–417. 2000. [Medline] [CrossRef]
16. Kumar O, Sugendran K, and Vijayaraghavan R. Oxidative stress associated hepatic and renal toxicity induced by ricin in mice. Toxicon. **41**(3): 333–338. 2003. [Medline] [CrossRef]
17. Pincus SH, Smallshaw JE, Song K, Berry J, and Vitetta ES. Passive and active vaccination strategies to prevent ricin poisoning. Toxins (Basel). **3**(9): 1163–1184. 2011. [Medline] [CrossRef]
18. Spilsberg B, Llorente A, and Sandvig K. Polyunsaturated fatty acids regulate Shiga toxin transport. Biochem Biophys Res Commun. **364**(2): 283–288. 2007. [Medline] [CrossRef]
19. Mukherjee S, and Maxfield FR. Role of membrane organization and membrane domains in endocytic lipid trafficking. Traffic. **1**(3): 203–211. 2000. [Medline] [CrossRef]
20. He X, McMahon S, Henderson TD 2nd, Griffey SM, and Cheng LW. Ricin toxicokinetics and its sensitive detection in mouse sera or feces using immuno-PCR. PLoS One. **5**(9): e12858. 2010. [Medline] [CrossRef]
21. Teahon K, Patel S, Menzies S, and Bjarnason I. Polyethylene glycol (PEG) 400 is unsuitable for assessing intestinal paracellular permeability. Gastroenterology. **104**: A283. 1993.
22. Mantis NJ, McGuinness CR, Sonuyi O, Edwards G, and Farrant SA. Immunoglobulin A antibodies against ricin A and B subunits protect epithelial cells from ricin intoxication. Infect Immun. **74**(6): 3455–3462. 2006. [Medline] [CrossRef]
23. Rubinstein A, Nakar D, and Sintov A. Chondroitin sulfate: a potential biodegradable carrier for colonic-specific drug delivery. Int J Pharm. **84**: 141–150. 1992. [CrossRef]
24. Teng Z, Yuan C, Zhang F, Huan M, Cao W, Li K, Yang J, Cao D, Zhou S, and Mei Q. Intestinal absorption and first-pass metabolism of polyphenol compounds in rat and their transport dynamics in Caco-2 cells. PLoS One. **7**(1): e29647. 2012. [Medline] [CrossRef]